

**Spectral control of emissions from
Sn-doped targets for EUV lithography**

S. S. Harilal, B. O'Shay, M. S. Tillack and Y. Tao

August 2005



Spectral control of emissions from Sn-doped targets for EUV lithography

S. S. Harilal, B. O'Shay, M. S. Tillack, Y. Tao,
University of California San Diego, Center for Energy Research,
9500 Gilman Drive, La Jolla, CA 92093-0438

R. Paguio², A. Nikroo² and C. A. Back²
²General Atomics, San Diego, CA 92186

We have investigated the unresolved transition array emission around 13.5 nm from solid density Sn and Sn doped foam targets. EUV emission measurements were made in the wavelength region 11-17 nm using a transmission grating spectrograph. The aim of this work was to optimize the UTA emission with the proper density of Sn dopant in low Z foam targets. It has been observed that the addition of Sn as an impurity in a low Z material leads to a reduction in the plasma continuum, narrowing the UTA compared to fully dense Sn targets. Our studies indicate that the required percentage of Sn for obtaining maximum efficiency at 13.5 nm is less than 1%.

Key words: Extreme ultraviolet lithography, EUV sources, laser-produced plasma

PACS: 52.38.-r, 52.38.Mf, 52.70.Kz

Extreme-ultraviolet (EUV) lithography is considered an attractive candidate to succeed conventional optical lithography in the coming years. To enable this technology, a reliable source will be required that consistently provides sufficient and clean power at 13.5 nm to yield adequate wafer throughput in a manufacturing tool. Researchers are considering various kinds of 13.5 nm sources including synchrotron radiation, discharge produced plasma, and laser-produced plasma¹. The advantages of using laser-produced plasma as a light are the power scalability through the tuning of laser parameters, high spectral purity, good dose control, spatial stability, minimal heat load, and a large solid angle of collection². A suitable scheme will require at least 3% conversion efficiency of incident laser energy to soft X-rays in a 2% bandwidth centered at the 13.5 nm peak. Different targets were considered for generating 13.5 nm plasma emission including lithium, xenon and tin. The success of an EUVL target depends not only upon its

emission characteristics at 13.5 nm but on the effective mitigation of its debris as well. Lithium plasma exhibits strong Lyman- α emission of Li^{2+} at 13.5 nm³. The conversion efficiency obtained with different Xe target plasmas is $\sim 1\%$ which is not enough for commercial lithography production purposes⁴. Laser-produced tin plasma is considered to be an ideal source for EUVL as it provides a conversion efficiency better than 3%⁵.

Tin plasmas characteristically emit broadband spectra around 13.5 nm that originate from many different ionization stages. These energy levels are so close that the radiation they generate in the EUV regime can be considered as a continuum (unresolved transition array, UTA). However, plasma from solid tin targets creates extreme debris problems. Apart from various particulates emitted from the plasma, the ions and neutrals which propagate with high expansion velocities ($\sim 1-3 \times 10^6$ cm/s) can damage the nearby optics in an EUVL system⁶. Several methods can be employed for limiting debris from the tin targets including electrostatic repeller fields⁷, the addition of ambient gas⁸, and application of magnetic fields⁹. Another method of restricting debris is to use the minimum amount of Sn atoms required for sufficient EUV emission¹⁰. It has been shown numerically that the tin ion distribution was not significantly changed when the concentration of tin dropped from 100% to 1%¹¹. Hayden et al.¹² found that targets containing 15% tin emit more brightly in the in-band region than fully dense tin targets. The aim of this study is to maximize the efficiency of EUV emission from tin doped foam targets while minimizing the number of tin atoms. Our results indicate that the density of tin necessary to obtain maximum efficiency at 13.5 nm is less than 1%. The use of low- Z material with tin atoms as an impurity will considerably reduce the recombination continuum around the EUV emitting region.

The targets were irradiated with 1064 nm, 10 ns pulses from an Nd:YAG laser focused with an $f/12$ antireflection coated plano-convex lens. The 60 μm diameter focal spot was measured using an optical imaging technique and remained unchanged during the experiment. The target was mounted in a vacuum chamber with a base pressure $\sim 10^{-6}$ Torr. EUV emission from the plasma was measured using a transmission grating spectrograph (TGS) equipped with a 10,000 lines/mm grating. The TGS was positioned at 45° with respect to the laser beam and employed a 50 μm slit to collimate incident

radiation onto the transmission grating. The dispersed spectra were recorded using a Princeton Instruments back illuminated x-ray CCD camera.

For fabricating the foam bead targets, the required amount of tin oxide is dispersed in a resorcinol formaldehyde (RF) solution and dried. The density of tin in the foam target is controlled by the concentration of tin in the solution. The target beads are ~ 500 microns in diameter, and the uniformity of the tin concentration was verified using a scanning electron microscope.

Four different targets were used in the present experiment which included a 10 μm solid density tin foil and tin doped foam targets of varying tin concentration (1%, 0.5% and 0.1%). A typical time integrated UTA recorded with our TGS for the 10 μm tin foil is given in Fig. 1. The spectral features of the 10 μm Sn foil were exactly like those of the solid Sn slab. The spectra were dominated by recombination continuum emission throughout the entire EUV. The UTA emission is concentrated around 13.5 nm with a narrow band gap of 5-10 eV arising from $4p^6 4d^n - 4p^5 4d^{n+1} + 4p^6 4d^{n-1} 4f$ transitions of various Sn ions ranging from Sn^{6+} to Sn^{14+} with occupancy in the range of $n = 2$ to $n = 8$ ^{11,13}. The laser intensity normalized CCD counts recorded at 13.5 nm as a function of laser power density is also given in Fig. 1 (inset). The variation of the normalized signal with laser power density shows that the maximum conversion efficiency occurs near our experimental value of $3.8 \times 10^{11} \text{ W/cm}^2$. Above the optimal laser irradiance, a greater portion of the radiated energy appears at shorter wavelengths, and at lower irradiance levels the plasma is insufficiently heated to emit at 13.5 nm. At the optimal laser irradiance level the ionization balance of the plasma shifts toward Sn^{9+} to Sn^{12+} which contributes primarily to in-band UTA radiation.

The EUV spectral energy from laser-produced tin plasma is significantly influenced by opacity effects. Tin plasma at 13.5 nm experiences attenuation of its strongest lines and is therefore optically thick¹⁴. In order to improve conversion efficiency it is important to facilitate the release of in-band plasma radiation. Fujikoa et. al.¹⁴ studied opacity effects and pointed out that for obtaining better conversion efficiency, the optical thickness of the tin plasma should be controlled by changing the initial target density. One of the most effective ways in accomplishing this is to use Sn atoms as a measurable impurity in the EUVL target.

Fig. 2 shows the UTA emission spectra from the 10 μm tin foil along with spectra from Sn doped foam targets of varying tin concentration. The laser intensity used was $3.8 \times 10^{11} \text{ W cm}^{-2}$ for all cases. The wavelength at which peak UTA intensity occurs is hardly affected by the percentage of Sn dopant. Compared to the solid Sn slab and Sn foil targets, the UTA emission from Sn doped foam targets showed reduced continuum emission and a narrowed spectrum peaked at 13.5 nm. It is reported that the presence of low Z elements with tin atoms will effectively reduce the average ionization state $\langle Z \rangle$ of the plasma, and hence the recombination continuum¹². Fujioka et. al.¹⁴ also observed similar narrowing of the UTA using low density targets and attributed it to a reduction of satellite emission from multiply excited Sn ions, and opacity broadening during the radiation transport. Theoretical calculations showed^{15,16} that the core tin ions contributing to the UTA at 13.5 nm range from Sn^{9+} - Sn^{12+} while lower charged species (Sn^{6+} - Sn^{8+}) emit at the longer wavelength side of the UTA ($>15 \text{ nm}$). Our results show that decreasing the tin density lead to the quenching of lower ionization states, and may be due to a reduction in the amount of cold plasma. It should be noted that the peak intensity around 13.5 nm did not change when the tin concentration dropped to 0.5%. In fact, the average peak intensity value over 10 shots (inset, Fig. 2) showed the highest brightness at 13.5 nm for the 0.5% tin doped foam compared to the 1% tin foam and 100% Sn foil. For full density tin targets there is considerable re-absorption of the radiation due to opacity effects, while a reduction in tin density results in an optically thin plasma. The 13.5 nm brightness of the 0.1% Sn target is lower than that of the other targets, and most likely due to the limited number of tin emitters ultimately resulting in poor efficiency.

The spectral features of Sn doped foam targets also contained oxygen emission lines. They are identified as O^{5+} lines at 12.99 nm (2p-4d) and 15.00 nm (2s-3p). Electron temperature is one of the most important parameters in determining the efficiency of the EUV emitting plasma since it determines the ion populations and ionization levels contributing to the UTA. Temperature of the tin doped foam targets was obtained using the intensity ratio of the O^{5+} lines by assuming local thermodynamic equilibrium (LTE)¹⁷. The estimated temperatures of the foam targets were $28.5 \pm 2.0 \text{ eV}$, $27.6 \pm 1.5 \text{ eV}$, and $18.0 \pm 2 \text{ eV}$ for 1%, 0.5%, and 0.1% tin doped foam respectively.

These represent the average temperature values of the EUV emitting plasma rather than defining the conditions at a particular stage of its evolution. Nevertheless, the reported optimum temperature required for better in-band conversion efficiency was $\sim 20 - 35$ eV which agrees well with estimated values¹¹.

We estimated the peak temperature and ionization level for different targets using HYADES - a one-dimensional radiation hydrodynamics plasma simulation code¹⁸. It should be emphasized that modeling the transient properties of a high Z plasma is a formidable task. The model has several limitations and specifically does not account for non-LTE behavior of the plasma, frequency dependent plasma opacity, atomic shell effects, or targets consisting of atomic mixtures. HYADES was used in planar geometry mode and due to the plane wave nature of the laser source, an input laser intensity of $\frac{1}{2}$ of the experimental value was specified. To simulate targets of reduced Sn concentration, we simply used a percentage of fully dense pure Sn. Peak electron temperature and charge state (using Saha ionization model) are plotted as a function of time in Fig. 3, and represent the bulk numerical zone behavior for the duration of the laser. For the 0.5% and 1% targets, there is very good agreement between the simulated peak electron temperature and that which was obtained from the O^{5+} spectral analysis. Moreover, the numerical results agree well with the reported plasma conditions for optimal conversion efficiency at 13.5 nm¹¹. However, as the concentration of Sn is lowered, the temperature and ionization state steadily increase, which is opposite to the trend observed in the experimental data. We believe this discrepancy is due to our inability to model the foam carrier (C,H,O mixture) of the Sn impurity atoms. The presence of the low Z atoms in the target would effectively reduce the plasma temperature and hence degree of ionization.

In summary, we have investigated the properties of EUV emission from laser created solid density Sn plasma and Sn doped foam plasmas. The spectral features showed that the EUV brightness was nearly the same within 10% fluctuation when the tin concentration was reduced from 100% to 0.5%. This implies that the optimal tin concentration required for EUV plasma emission is less than 1%. The EUV emission from tin doped targets also showed better contrast between in-band and out of band radiation with narrower UTA spectral profiles. This indicates that the reduction of Sn

density leads to a quenching of the population of lower ionization states as well as the plasma continuum. The spectral narrowing will definitely reduce the thermal loading to EUV collection optics since a reduced bandwidth spectrum would fall onto the multi-layer mirrors in the lithographic system.

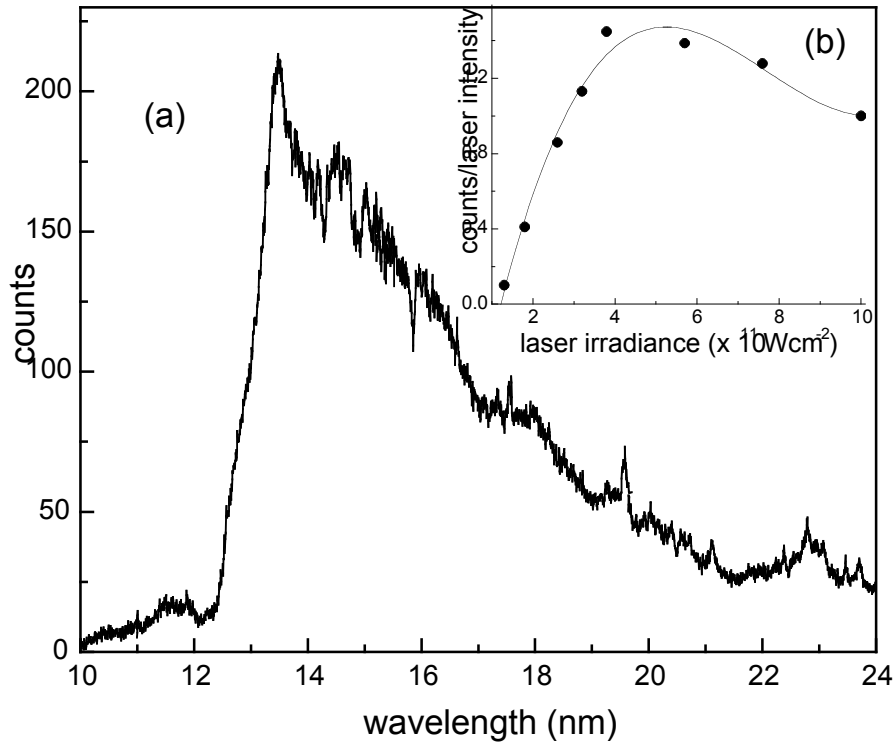


Fig. 1. UTA emission from 10 μm tin foil (a). Normalized UTA brightness variation with laser intensity at 13.5 nm is given in the inset (b). The curve represents the best fit to data.

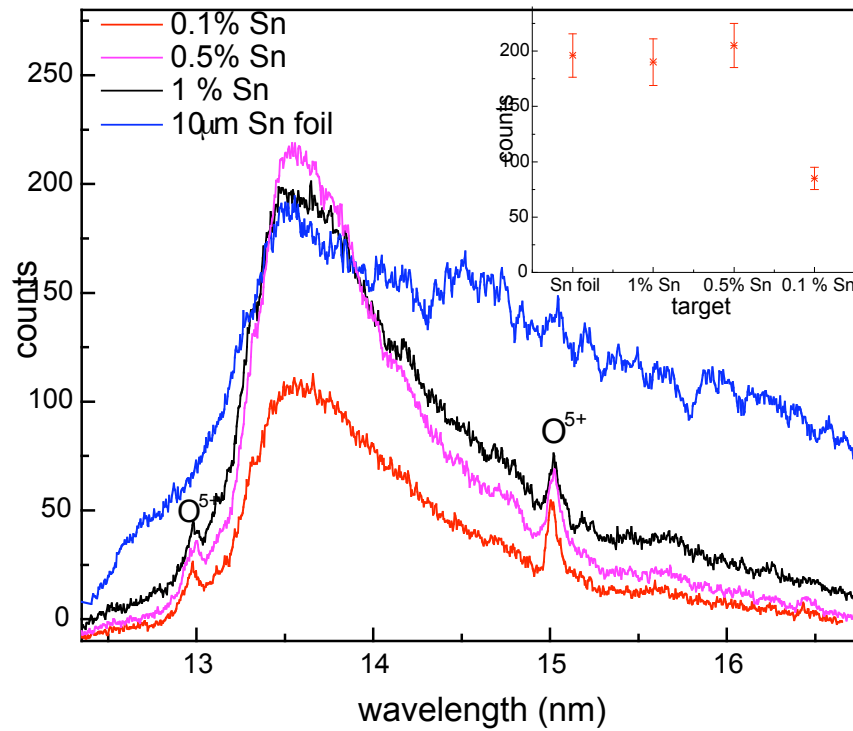


Fig.2. Typical UTA spectra from Sn foil target and Sn doped foam targets. The figure in the inset shows the average peak counts at 13.5 nm for various targets used.

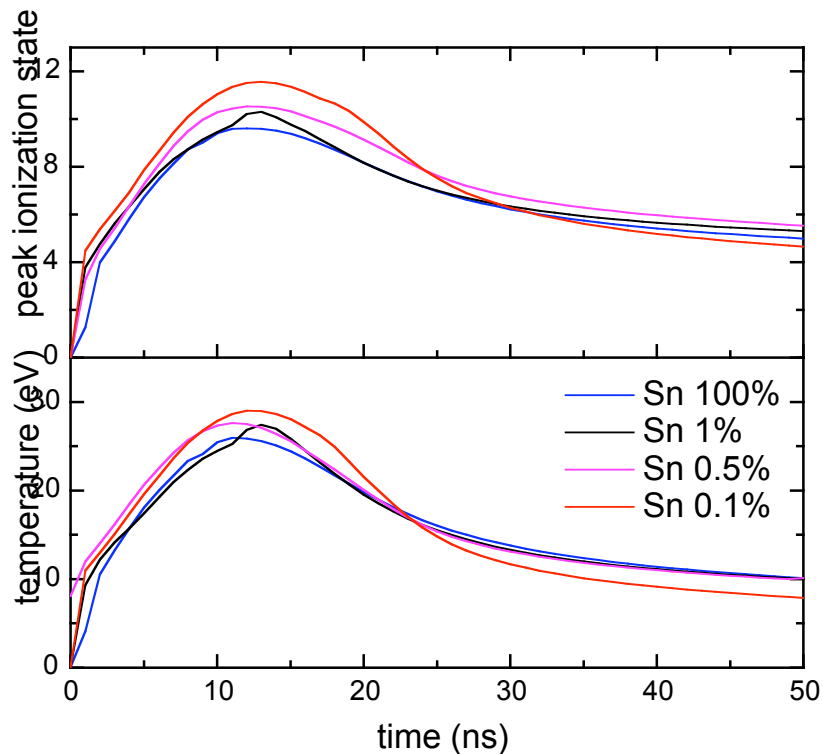


Fig.3. The peak temperature and ionization values obtained for different targets with HYADES simulation code.

¹D. W. Myers, I. V. Fomenkov, W. Partlo, D. C. Brandt, and B. C. Klene, *Solid State Technology* **48**, 67 (2005).

²B. Marx, *Laser Focus World* **39**, 34 (2003).

³T. Higashiguchi, C. Rajyaguru, S. Kubodera, W. Sasaki, N. Yugami, T. Kikuchi, S. Kawata, and A. Andreev, *Applied Physics Letters* **86**, 231502 (2005).

⁴M. Miyamoto, A. Shimoura, S. Amano, K. Fukugaki, H. Kinugasa, T. Inoue, and T. Mochizuki, *Applied Physics Letters* **86**, 261502 (2005).

⁵Y. Shimada, H. Nishimura, M. Nakai, K. Hashimoto, M. Yamaura, Y. Tao, K. Shigemori, T. Okuno, K. Nishihara, T. Kawamura, A. Sunahara, T. Nishikawa, A. Sasaki, K. Nagai, T. Norimatsu, S. Fujioka, S. Uchida, N. Miyanaga, Y. Izawa, and C. Yamanaka, *Applied Physics Letters* **86**, 051501 (2005).

- ⁶S. S. Harilal, B. O'Shay, M. S. Tillack, and M. V. Mathew, *Journal of Applied Physics* **98**, (in press) (2005).
- ⁷K. Takenoshita, C. S. Koay, S. Teerawattanasook, M. Richardson, and V. Bakshi, *Proc. of SPIE* **5751**, 563 (2005).
- ⁸F. Flora, L. Mezi, C. E. Zheng, and F. Bonfigli, *Europhysics Letters* **56**, 676 (2001).
- ⁹S. S. Harilal, B. O'Shay, and M. S. Tillack, *Journal of Applied Physics* **98**, in press (2005).
- ¹⁰M. Richardson, C. S. Koay, K. Takenoshita, C. Keyser, and M. Al-Rabban, *Journal of Vacuum Science & Technology B* **22**, 785 (2004).
- ¹¹A. Cummings, G. O'Sullivan, P. Dunne, E. Sokell, N. Murphy, and J. White, *Journal of Physics D-Applied Physics* **38**, 604 (2005).
- ¹²P. Hayden, A. Cummings, L. Gaynor, N. Murphy, G. O'Sullivan, P. Sheridan, E. Sokell, J. White, and P. Dunne, *Proc. of SPIE* **5751**, 919 (2005).
- ¹³G. Osullivan and R. Faulkner, *Optical Engineering* **33**, 3978 (1994).
- ¹⁴S. Fujioka, H. Nishimura, T. Okuno, Y. Tao, N. Ueda, T. Ando, H. Kurayama, Y. Yasuda, S. Uchida, Y. Shimada, M. Yamaura, Q. Gu, K. Nagai, T. Norimatsu, H. Furukawa, A. Sunahara, Y. Kang, M. Murakami, K. Nishihara, N. Miyanaga, and Y. Izawa, *Proc. of SPIE* **5751**, 578 (2005).
- ¹⁵A. Sasaki, K. Nishihara, F. Koike, T. Kagawa, T. Nishikawa, K. Fujima, T. Kawamura, and H. Furukawa, *IEEE J. Selected Top. Quan. Electr.* **10**, 1307 (2004).
- ¹⁶A. Ryabtsev, I. Tolstihina, S. Churilov, and K. Koshelev, *Sn data for EUV sources*, Sematech EUV Source workshop, Miyazaki, Japan, 2004.
- ¹⁷H. R. Griem, *Principles of Plasma Spectroscopy* (Cambridge, New York, 1997).
- ¹⁸J. T. Larsen and S. M. Lane, *Journal of Quantitative Spectroscopy & Radiative Transfer* **51**, 179 (1994).